Experimental Demonstration of Relativistic Self-Channeling of a Multiterawatt Laser Pulse in an Underdense Plasma

P. Monot, T. Auguste, P. Gibbon, F. Jakober, and G. Mainfray

Commissariat a L'Énergie Atomique Direction des Sciences de la Matière Département de Recherche sur L'État Condensé, Les Atomes et Les Molécules, Bâtiment 522, C.E. Saclay, 91191 Gif sur Yvette Cedex, France

A. Dulieu, M. Louis-Jacquet, G. Malka, and J. L. Miquel

Commissariat a L'Énergie Atomique, DAM/DLPP/EPL, C.E. Limeil-Valenton, 94195 Villeneuve St. Georges Cedex, France

(Received 2 September 1994)

We report the first clear experimental demonstration of relativistic self-channeling of a multiterawatt laser pulse interacting with an underdense plasma. We show via Thomson scattering observations that for laser power above the critical power for self-focusing the beam remains trapped and guided over the plasma length. These observations are in fairly good agreement with a numerical model describing the laser propagation and taking into account the plasma response to the ponderomotive force.

PACS numbers: 52.40.Nk, 42.50.Rh, 52.35.Mw, 52.40.Db

With the advent of a new class of compact short-pulse terawatt laser systems, focused intensities as high as 10^{18} W/cm^2 are now routinely achieved, and it has become possible to explore relativistic laser-matter interaction.

One of the most promising topics of investigation is relativistic self-focusing and self-channeling of an intense electromagnetic wave in a plasma. This phenomenon is particularly interesting because it is an attractive way to achieve intensities which have not been reached by conventional means (lenses or mirrors) until now. Second, it is of great interest for processes requiring long length interaction such as laser-plasma-based electron accelerators [1] or optical-field ionization x-ray lasers [2]. Numerous theoretical works have been devoted to this subject [3], and it is now generally believed that self-focusing and self-channeling in a homogeneous medium should occur for incident laser powers P exceeding a particular value known as the critical power, given by $P_c = 17(\omega^2/\omega_p^2)$ GW where ω is the laser frequency, $\omega_p = 5.64 \times 10^4 \times [N_e\ (\mathrm{cm}^{-3})]^{1/2}\ \mathrm{s}^{-1}$ is the plasma frequency, and N_e is the electron density.

Basically, relativistic self-focusing arises from an increase of electron inertia under the action of the intense electromagnetic (e.m.) wave. This increase of electron mass induces an increase of the index of refraction of the plasma which is given by

$$n = \sqrt{1 - \omega_p^2/\gamma\omega^2}, \tag{1}$$

where γ is the relativistic factor. Because the e.m. wave is focused, the plasma index of refraction is peaked on the laser beam axis where the intensity has a maximum. The plasma is thus a positive lens. When $P < P_c$, beam divergence is reduced. For $P = P_c$, the modification of the plasma index of refraction due to the relativistic effect exactly cancels beam diffraction, and the e.m. wave can be guided over distances much larger than the Rayleigh length. For $P > P_c$, self-focusing takes place.

For the maximum laser power presently available, an electron density close to 10^{19} cm^{-3} is required. The simplest way to achieve such a high-density plasma is to ionize a gas medium with the laser itself. To date, most of the experiments reporting observations of extended propagation were performed by focusing the laser into a static-filled target chamber [4,5] with a pressure up to 5 atm [4]. Under these conditions, it has been shown [6–8] that ionization-induced defocusing drastically reduces the peak intensity from its vacuum value and therefore limits the maximum achievable plasma density. In the experiment reported herein, this defocusing effect has been prevented by using a hydrogen gas jet [9]. The laser was focused at the vacuum-gas interface in order to obtain both a high laser intensity and a high electron density.

In this Letter, we present experimental results for incident laser powers up to $5P_c$. We demonstrate that for $P < P_c$, the laser beam is focused over two Rayleigh lengths, i.e., over the confocal parameter ($b = 2z_R \approx 0.6$ mm), whereas for $P > P_c$, the beam remains guided over the plasma length ($L_p \approx 3$ mm). We use a simple propagation model including the plasma dynamics to *infer* the maximum focused intensity reached in the ionized medium. We find that it can exceed by at least a factor of 5 the focused intensity in vacuum.

The P102 terawatt laser used has already been described [10]. Briefly, it is based on the chirped-pulse amplification technique and operates at $\lambda = 1058$ nm. The pulse generated by a Ti-sapphire femtosecond laser is temporally stretched and then goes into a Ti-sapphire regenerative amplifier. It is further amplified in Nd silicate and phosphate rods up to 24 J and temporally compressed down to 400 fs. The maximum power available was 55 TW, but for the experiment reported herein the power was limited to 15 TW, first to avoid beam filamentation in air, which may occur when the multiterawatt pulse propagates from the compression stage to the

interaction chamber, and second to keep a smooth near-Gaussian focused intensity profile. The maximum intensity measured in vacuum is about 3×10^{18} W/cm^2 for a 15-TW laser power.

The plasma is created by focusing the 90-mm-diam beam with a 635 mm focal-length lens onto a pulsed hydrogen jet. The neutral gas density measured with a Wollaston interferometer [9] has a 1×3 mm^2 flat-top profile. The laser propagates along the 3 mm length. A maximum electron density of 10^{19} cm^{-3} was achieved in this experiment. The H_2 molecule is ionized and dissociated in the rising edge of the laser pulse once the intensity exceeds 10^{14} W/cm^2 [11]. Hence, most of the pulse experiences a plasma consisting only of electrons and protons and exhibiting homogeneous initial radial density profiles. The use of both molecular hydrogen and a jet configuration avoids premature refraction of the laser beam by the plasma [9].

In order to study the propagation of the laser in plasma we measured the Thomson scattered laser light at 90° to the propagation direction. An image of the focal region is produced onto a charged-coupled-device (CCD) camera connected to a computer. The spatial resolution is limited by the pixel size which is 12×16 μm^2. The laser radiation was selected with a 10 nm full width at half maximum (FWHM) interferential filter.

Figure 1 shows Thomson longitudinal profiles obtained for a 2.5×10^{18} cm^{-3} electron density. This gives a 6.8 TW critical power for self-focusing. The laser is focused at the entrance of the gas jet and propagates from the left to the right of the figure. The curve drawn with dashed lines is obtained for a 1 TW incident laser power, and the scattering region extends over 1.2 mm which corresponds to a beam propagation similar to that in vacuum. The solid line corresponds to a 10 TW laser power, and the scattered-light profile FWHM (L_z) is as large as the plasma length (L_p), which is limited by the 3 mm jet size. The curve exhibits two maxima spaced by about 2 mm.

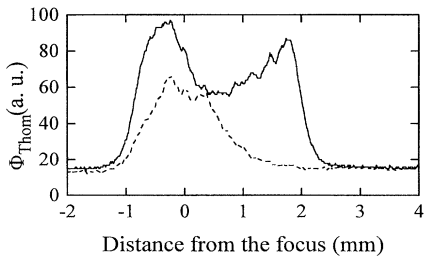

FIG. 1. Experimental axial Thomson profiles taken along the laser propagation axis and measured for a 2.5×10^{18} cm^{-3} electron density, i.e., for $P_c = 6.8$ TW. The laser propagates from the left to the right of the figure. The curve drawn with dashed lines is obtained for $P = 1$ TW. The solid curve is taken for $P = 10$ TW.

In order to interpret such a behavior, we have used a steady-state propagation model similar to that described in Ref. [12] which is based on a standard paraxial wave equation,

$$\frac{\partial a}{\partial z} + \frac{i}{2v_g}\left(\nabla_\perp^2 + N_{e0} - \frac{N_e}{\gamma}\right)a = 0, \qquad (2)$$

where $v_g = (1 - \omega_p^2/\omega^2)^{1/2}$ is the normalized group velocity. The spatial coordinates r and z are normalized to k^{-1} where k is the laser wave vector. The vector potential $\mathbf{a}$ is normalized to the Compton potential $m_e c^2/e$. Assuming the plasma response is adiabatic ($\partial/\partial t \ll \omega_p$), then combining the Lorentz and Poisson equations we can write $N_e = N_{e0} + \nabla_\perp^2 \gamma$, the second term arising from the radial charge separation due to the ponderomotive force. N_{e0} is the unperturbed electron density. N_e and N_{e0} are normalized to the critical density N_c, the maximum density above which radiation of a given wavelength λ cannot propagate. For $\lambda = 1$ μm, $N_c = 10^{21}$ cm^{-3}. The relativistic factor γ is given by

$$\gamma = (1 + |\mathbf{a}|^2/2)^{1/2}. \qquad (3)$$

This expression for γ is exact to $O(\omega_p/\omega)^2|\mathbf{a}|^4$.

We must emphasize that experimental scattered-light profiles are not *directly* comparable with numerical calculations of the laser spatiotemporal intensity distribution because the Thomson scattered radiation depends on the *product* of the intensity distribution and the electron density profile. In other words, the image of the scattering region is not *necessarily* the image of the laser beam, especially in an inhomogeneous medium.

A comparison with experiments can nonetheless be made by integrating the product of the radial intensity shape times the electron density profile along the observation axis [13]. Assuming all quantities are axisymmetric, the Thomson profile along the chords $y = \text{const}$ is given by

$$\Phi_{\text{Thom}}(y,z) \alpha \int_y^R \frac{N_e(r,z)}{\gamma^2(r,z)} \frac{I(r,z)}{\sqrt{r^2 - y^2}}\, r\, dr, \qquad (4)$$

where $I(r,z) = |\mathbf{a}(r,z)|^2$ is the normalized intensity and R is the plasma radius. Such a calculation of Thomson signal is only valid for incoherent scattering. By varying the gas pressure, we verified experimentally that the scattered light intensity depends linearly upon electron density, which gives us confidence in Eq. (4).

Figure 2(a) shows on-axis ($y = 0$) Thomson signals calculated for the same conditions as in Fig. 1. One can see that there is a fairly good agreement between experimental and numerical results. Figure 2(b) shows the on-axis longitudinal laser intensity distributions. For $P < P_c$, the focused laser intensity in the plasma (drawn with dashed lines) is the same as in vacuum, i.e., 3×10^{17} W/cm^2 while for $P > P_c$, the intensity is six times that reached in vacuum ($I_{\max} = 1.8 \times 10^{19}$ W/cm^2). Note also that, for $P < P_c$, Thomson signal and intensity

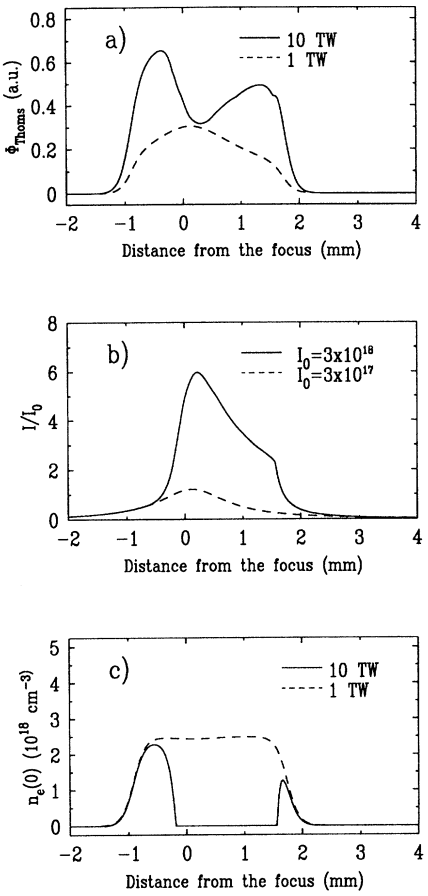

FIG. 2. On-axis (a) Thomson profiles, (b) intensity profiles, and (c) electron density profiles calculated for laser powers and focal geometry relevant to experimental conditions of results shown in Fig. 1. Dashed line: $P < P_c$ ($I_{max} = I_0 = 3 \times 10^{17}$ W/cm^2). Solid line: $P > P_c$ ($I_{max} = 6I_0 = 1.8 \times 10^{19}$ W/cm^2). For convenience, the Thomson signal corresponding to $P < P_c$ has been multiplied by a factor of 30.

maxima coincide, whereas for $P > P_c$, the scattered light is minimum where the laser intensity is maximum. This feature arises from the fact that, when the incident laser power is kept well below the critical power for self-focusing, the ponderomotive force is insufficient to expel electrons, and the density distribution, represented by dashed lines in Fig. 2(c), remains homogeneous. On the other hand, when the laser power exceeds the critical power, electrons are pushed out of the focal volume by the enhanced ponderomotive force resulting from self-focusing, and the density distribution becomes inhomogeneous as seen by the solid curve in Fig. 2(c).

Figure 3 shows experimental axial Thomson profiles taken for $N_e = 8 \times 10^{18}$ cm^{-3} ($P = 5P_c$) and $N_e = 10^{19}$ cm^{-3} ($P = 6P_c$), respectively. We comment first on the result obtained for $P = 5P_c$ (dashed line). The comparison with the solid curve of Fig. 1 shows that

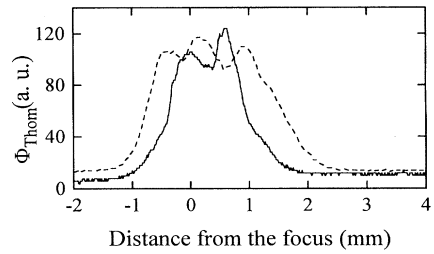

FIG. 3. Experimental axial Thomson profiles taken along the laser propagation axis and measured for $N_e = 8 \times 10^{18}$ cm^{-3}, $P = 10$ TW, i.e., for $P = 5P_c$ (dashed line) and for $N_e = 10^{19}$ cm^{-3}, $P = 10$ TW, i.e., for $P = 6P_c$ (solid line).

the number of ripples in the profile grows when P/P_c is increased and the spacing between them decreases. The axial extension of the scattering zone also becomes shorter than the plasma length ($L_z \approx 2.5$ mm). Extrapolating the relationship between Thomson and intensity profiles established for the data of Fig. 1, the shape of the scattered-light curve suggests that successive foci are formed before the beam leaves the plasma. The scattering region is even shorter when increasing the electron density to 10^{19} cm^{-3} (Fig. 3, solid line) ($L_z \approx 1.5$ mm) and only two emission peaks spaced by 600 μm remain on the Thomson profile, the amplitude of the second peak being higher than that of the first peak. The beam probably gets strongly self-focused before blowing up. This result is in good agreement with theoretical considerations [3]: When the beam is strongly self-focused so that the beam spot size becomes comparable to the wavelength, the diffraction term of the propagation equation is responsible for a strong spreading of the e.m. field.

Figure 4 shows calculated profiles for the same conditions as in Fig. 3. A comparison of the dashed curves in Figs. 3 and 4 shows that a qualitative agreement is still found between experimental and calculated Thomson profiles for $P = 5P_c$. The number of emission peaks and their spacing is quite well described by the calculations, which also predict a 4×10^{19} W/cm^2 ($I_{max} = 14I_0$) max-

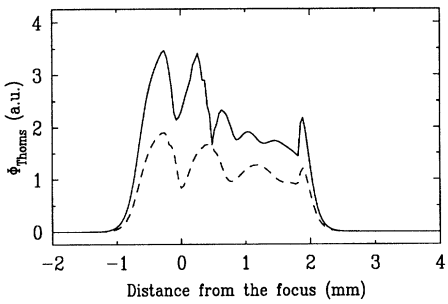

FIG. 4. Calculated axial Thomson profiles obtained for laser powers and focal geometry relevant to experimental conditions of results shown in Fig. 3. Dashed line: $P = 5P_c$. Solid line: $P = 6P_c$.

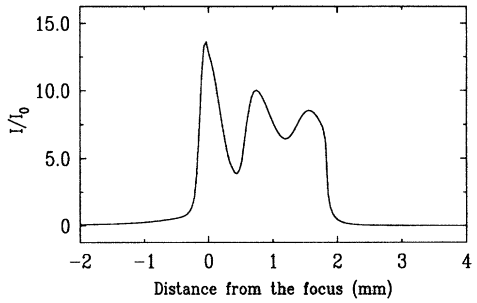

FIG. 5. On-axis longitudinal intensity profile corresponding to Thomson profile drawn with dashed lines in Fig. 3 ($P = 5P_c$). The intensity in the three peaks is 4×10^{19}, 3×10^{19}, and 2.5×10^{19} W/cm^2, respectively. $I_0 = 3 \times 10^{18}$ W/cm^2. The spacing between two successive maxima is about 750 μm.

imum intensity on axis followed by two secondary peaks with intensities $I = 3 \times 10^{19}$ and 2.5×10^{19} W/cm^2, respectively (Fig. 5). Peaks are equally spaced from each other by approximately 750 μm. This periodic structure is a general feature of beam propagation in a nonlinear medium [14] with a power in excess of the critical power for self-focusing. This arises from a competition between diffraction and self-focusing terms in the propagation equation. The beam radius oscillates around a value for which diffraction and self-focusing terms exactly cancel each other. One can also see that the more the laser power exceeds the critical power, the more numerical simulations tend to deviate from experimental results in the right edge of the profile. As an example, for $P = 6P_c$, experimental data (Fig. 3, solid line) and numerical calculations (solid line in Fig. 4) are in good agreement in the first part of the profile while the latter part exhibits significant differences. Such a discrepancy may arise from the fact that calculations are performed under the paraxial approximation, which assumes that $k_\perp \ll k$, where $k_\perp$ is the wave vector of a transverse mode. In vacuum, $k_\perp \sim w_0^{-1}$ where w_0 is the beam waist. For $P = 6P_c$, the numerical calculation gives a 0.5 μm minimum beam radius, which would imply $k_\perp > k$, and the paraxial approximation breaks down.

Another possible reason for the discrepancy is the expulsion of ions from the channel via the space-charge field $E_\perp = -\nabla_\perp \gamma$. In the strongly relativistic limit, one can estimate the expulsion time as [15]

$$\Delta t_i \approx 140 \sigma_\mu (I_{18} \lambda_\mu^2)^{-1/4} \text{ fs}, \quad (5)$$

where σ_μ is the focused beam radius in microns and I_{18} is the laser focused intensity in units of 10^{18} W/cm^2. From the numerical solutions of Figs. 2 and 5 we have $\Delta t_i \approx$ 300 and 100 fs, respectively. Since the pulse length was 400 fs, we would certainly expect worsening agreement with increasing P/P_c. Finally, we note that the front and rear of the pulse will exhibit different focusing behavior to the pulse center for $P > P_c$, which would have a smoothing effect on the measured Thomson signal.

In conclusion, we demonstrated that relativistic self-focusing and self-channeling of the laser beam occur when P is in the $(1.5–5)P_c$ range. A maximum laser intensity of 5–15 times that reached in vacuum has been inferred from numerical solutions of the paraxial wave equation up to a limiting case where the paraxial approximation breaks down. For $P = 5P_c$, a periodic structure appeared in the Thomson signal, suggesting multiple foci formation.

The authors wish to acknowledge the assistance of I. Allais, C. Martin, E. Mazataud, A. Pierre, and C. Rouyer.

[1] E. Esarey *et al.*, Phys. Fluids B **5**, 2690 (1993).
[2] N. H. Burnett and G. D. Enright, IEEE J. Quantum Electron. **26**, 1797 (1990); P. Amendt, D. C. Eder, and S. C. Wilks, Phys. Rev. Lett. **66**, 2589 (1991).
[3] C. E. Max, J. Arons, and A. B. Langdon, Phys. Rev. Lett. **33**, 209 (1974); P. Sprangle, C. M. Tang, and E. Esarey, IEEE Trans. Plasma Sci. **15**, 145 (1987); G. Z. Sun, E. Ott, Y. C. Lee, and P. Guzdar, Phys. Fluids **30**, 526 (1987); H. S. Brandi *et al.*, Phys. Fluids **5**, 3539 (1993).
[4] A. B. Borisov *et al.*, Phys. Rev. Lett. **68**, 2309 (1992).
[5] R. W. Falcone, in *X-Ray Lasers*—1992, edited by E. E. Fill, IOP Conf. Proc. No. 125 (Institute of Physics and Physical Society, London, 1992), p. 213.
[6] P. Monot *et al.*, J. Opt. Soc. Am. B **9**, 1579 (1992).
[7] S. C. Rae, Opt. Commun. **97**, 25 (1993).
[8] E. E. Fill, J. Opt. Soc. Am. B **11**, 2241 (1994).
[9] T. Auguste *et al.*, Opt. Commun. **105**, 292 (1994).
[10] C. Rouyer *et al.*, Opt. Lett. **18**, 214 (1993).
[11] C. Cornaggia *et al.*, Phys. Rev. A **34**, 207 (1986).
[12] A. B. Borisov *et al.*, Phys. Rev. Lett. **65**, 1753 (1990).
[13] P. Gibbon *et al.*, Phys. Plasmas (to be published).
[14] Y. R. Shen, *The Principle of Non-linear Optics* (Wiley, New York, 1984).
[15] W. B. Mori *et al.*, Phys. Rev. Lett. **60**, 1298 (1988).